Synergistic Regulation of the Co Microenvironment in MOF-74 for Olefin Epoxidation via Lanthanum Modification and Defect Engineering

Chang'an Wang [a], Zuoshuai Xi [a], Tao Ban [a], Zhiyuan Liu [a], Yibin Luo [b], Hongyi Gao [a, *], Ge Wang [a, *], Xingtian Shu [b, *]

a Beijing Advanced Innovation Center for Materials Genome Engineering, Beijing Key Laboratory of Function Materials for Molecule & Structure Construction, School of Materials Science and Engineering, University of Science and Technology Beijing, Beijing 100083, PR China.

b Sinopec Research Institute of Petroleum Processing Co., Ltd, Beijing 100083, PR China.

*Corresponding author at: School of Materials Science and Engineering, University of Science and Technology Beijing, Beijing 100083, PR China.

*Corresponding Authors:

E-mail addresses: hygao@ustb.edu.cn; gewang@ustb.edu.cn; shuxingtian.ripp@sinopec.com.

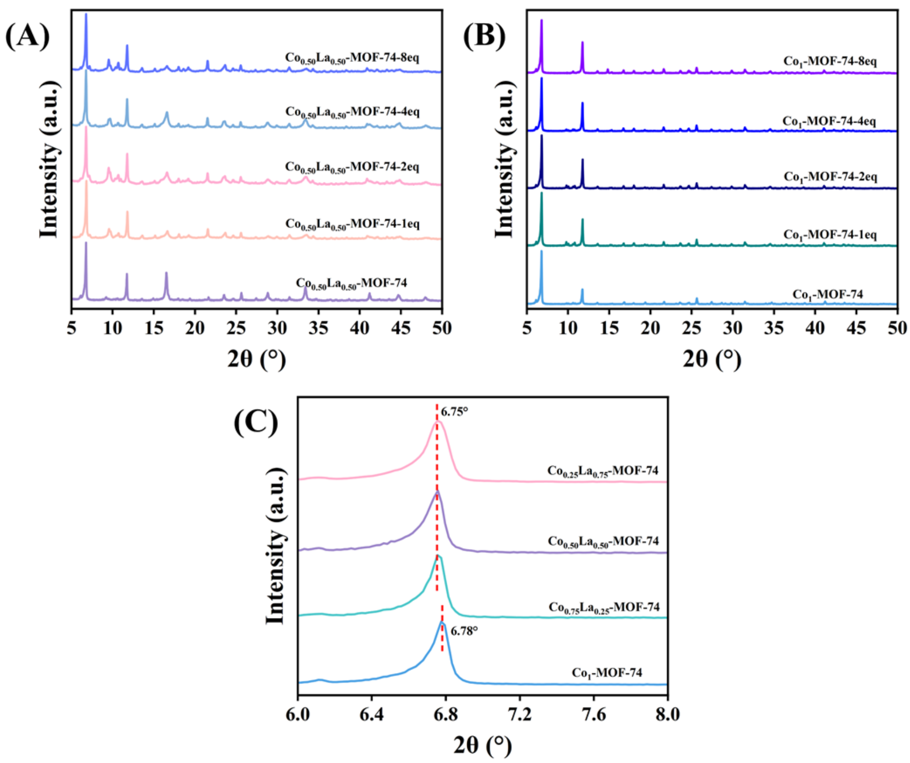

Figure S1. XRD patterns of (A) $Co_{0.50}La_{0.50}$-MOF-74 and $Co_{0.50}La_{0.50}$-MOF-74-xeq, (B) Co_1-MOF-74-xeq. (C) Partial enlarged patterns of Co_xLa_{1-x}-MOF-74 at 6.0-8.0°.

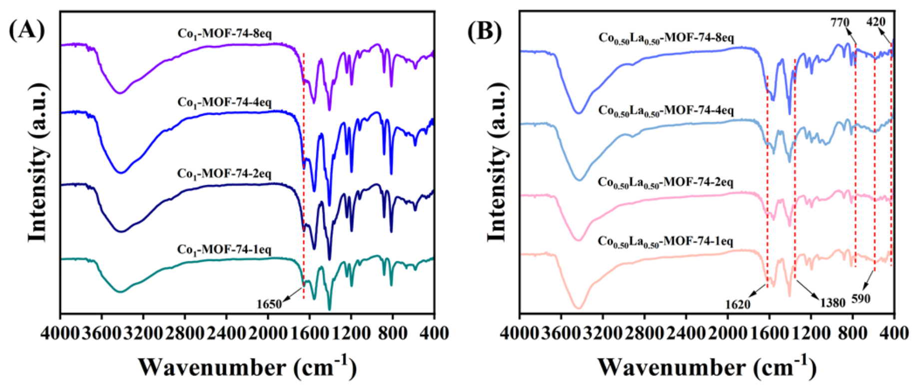

Figure S2. FT-IR patterns of (A) Co_1-MOF-74-xeq and (B) $Co_{0.50}La_{0.50}$-MOF-74-xeq.

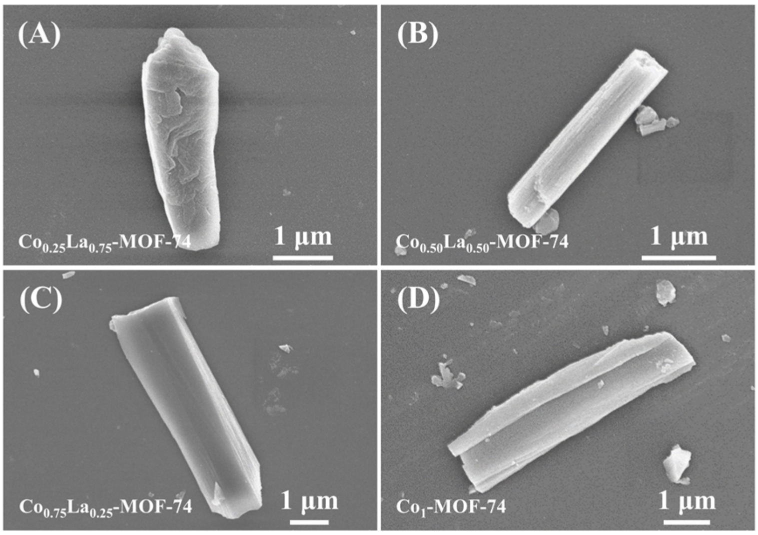

Figure S3. SEM images of (A) $Co_{0.25}La_{0.75}$-MOF-74, (B) $Co_{0.50}La_{0.50}$-MOF-74, (C) $Co_{0.75}La_{0.25}$-MOF-74 and (D) Co_1-MOF-74.

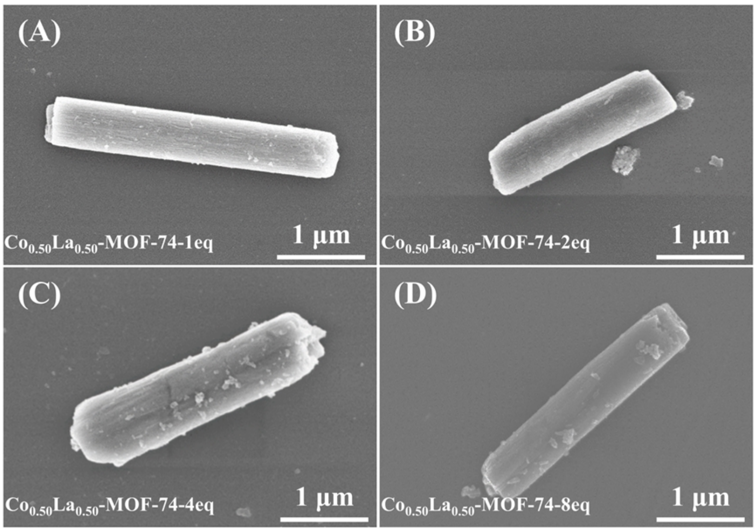

Figure S4. SEM images of (A) $Co_{0.50}La_{0.50}$-MOF-74-1eq, (B) $Co_{0.50}La_{0.50}$-MOF-74-2eq, (C) $Co_{0.50}La_{0.50}$-MOF-74-4eq and (D) $Co_{0.50}La_{0.50}$-MOF-74-8eq.

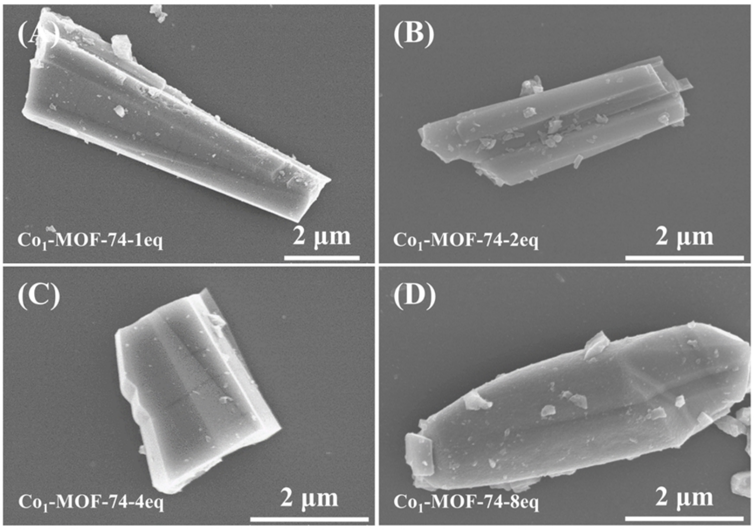

Figure S5. SEM images of (A) Co_1-MOF-74-1eq, (B) Co_1-MOF-74-2eq, (C) Co_1-MOF-74-4eq and (D) Co_1-MOF-74-8eq.

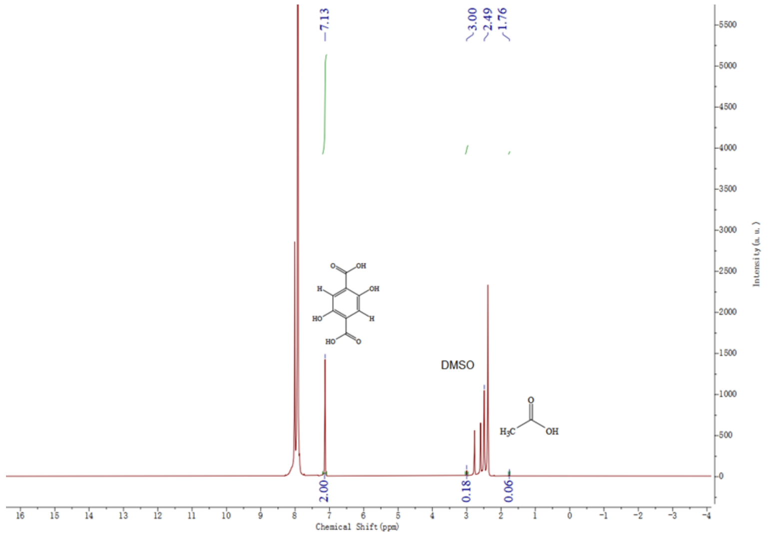

Figure S6. [1]H NMR spectrum of $Co_{0.50}La_{0.50}$-MOF-74-1eq.

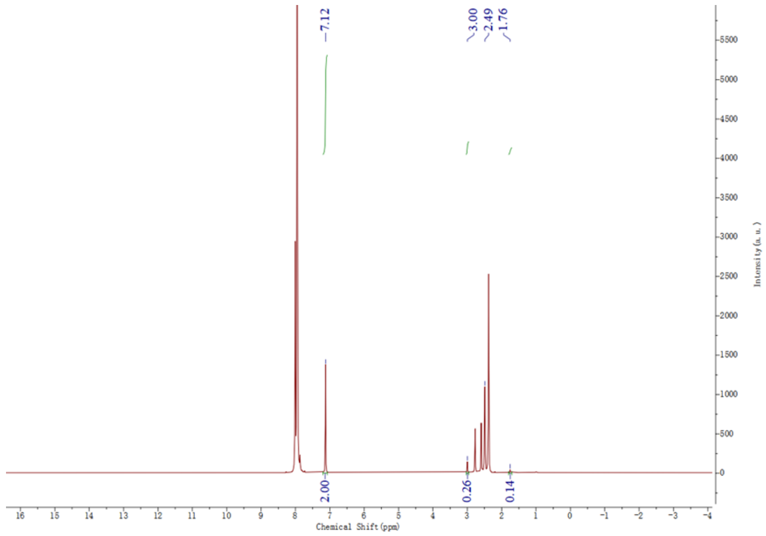

Figure S7. ^{1}H NMR spectrum of $Co_{0.50}La_{0.50}$-MOF-74-2eq.

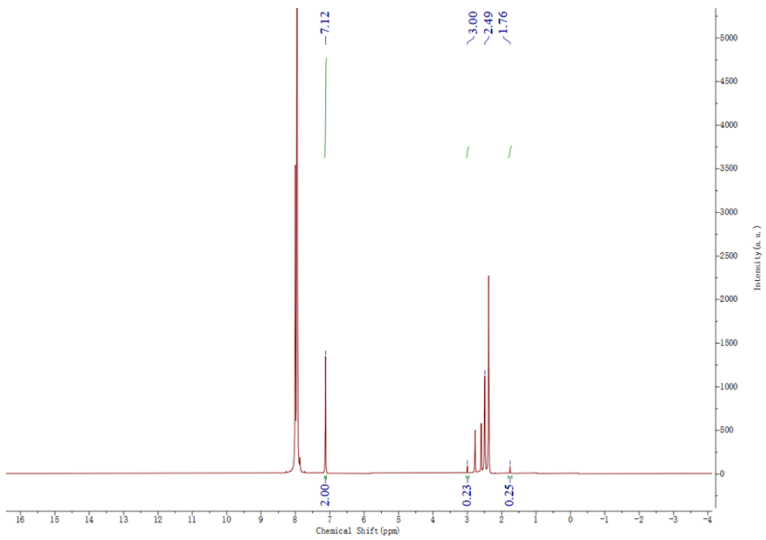

Figure S8. ^{1}H NMR spectrum of $Co_{0.50}La_{0.50}$-MOF-74-4eq.

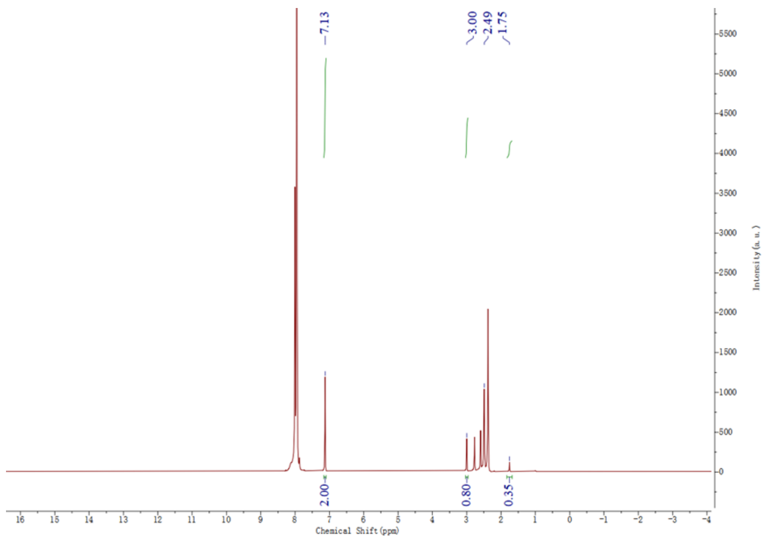

Figure S9. ^{1}H NMR spectrum of $Co_{0.50}La_{0.50}$-MOF-74-8eq.

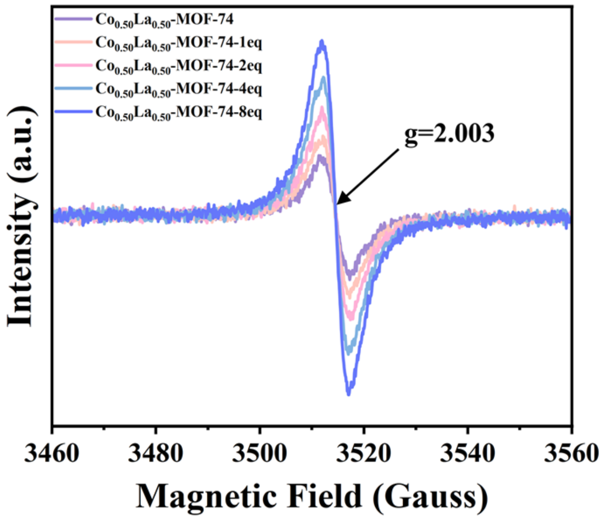

Figure S10. EPR spectra of $Co_{0.50}La_{0.50}$-MOF-74 and $Co_{0.50}La_{0.50}$-MOF-74-xeq.

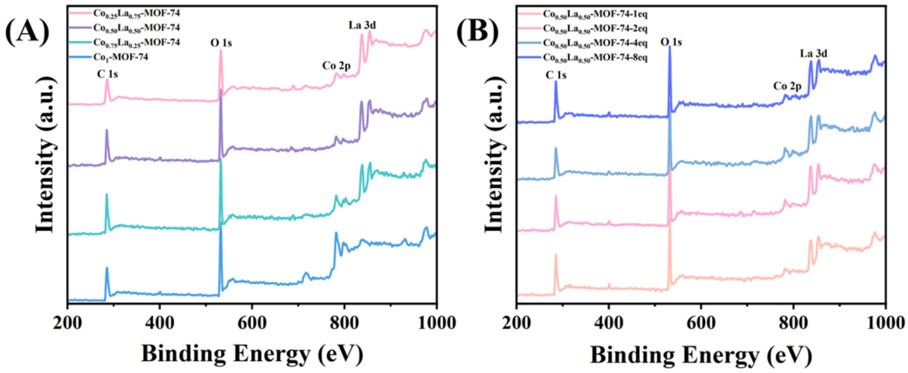

Figure S11. XPS survey spectra of (A) Co_xLa_{1-x}-MOF-74 and (B) $Co_{0.50}La_{0.50}$-MOF-74-xeq.

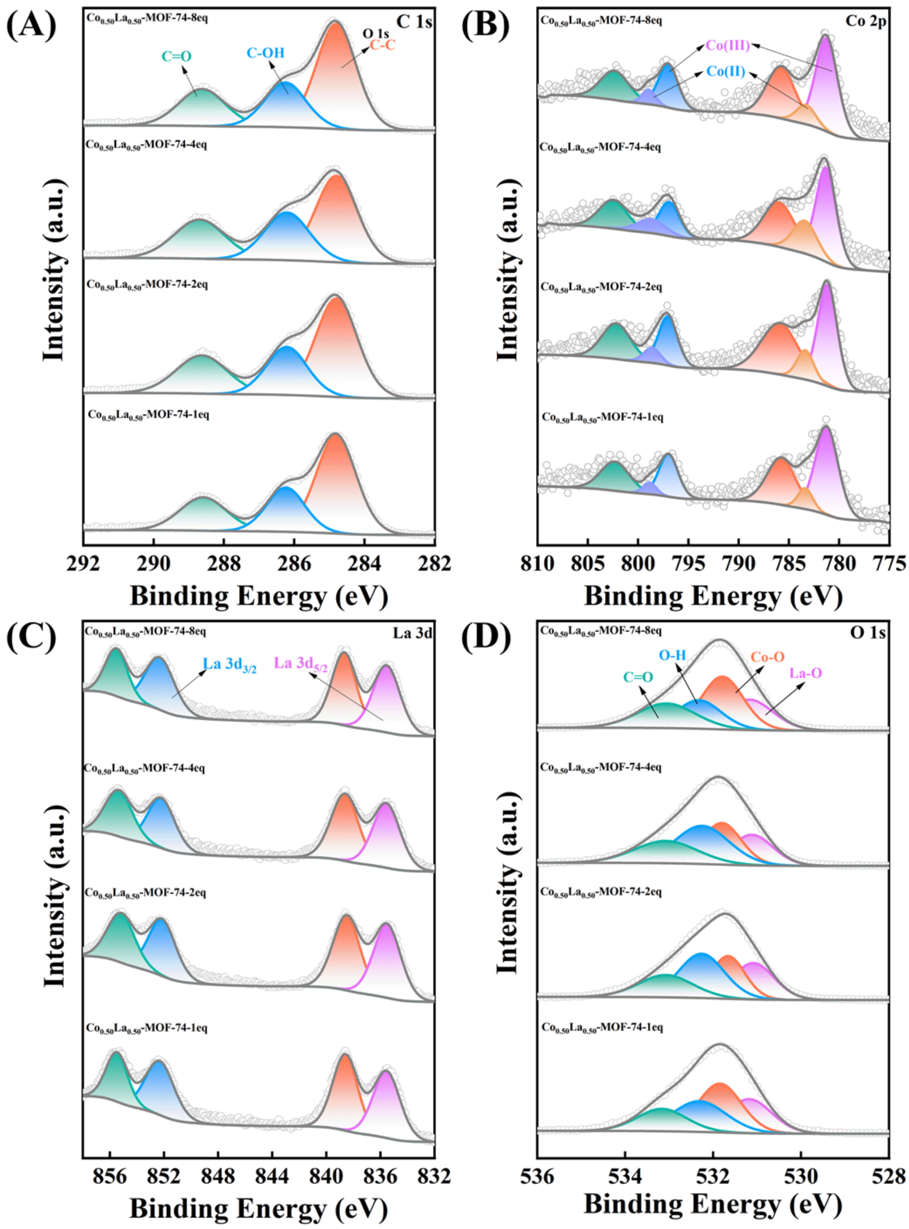

Figure S12. High-resolution XPS spectra of (A) C 1s, (B) Co 2p, (C) La 3d and (D) O 1s in $Co_{0.50}La_{0.50}$-MOF-74-xeq.

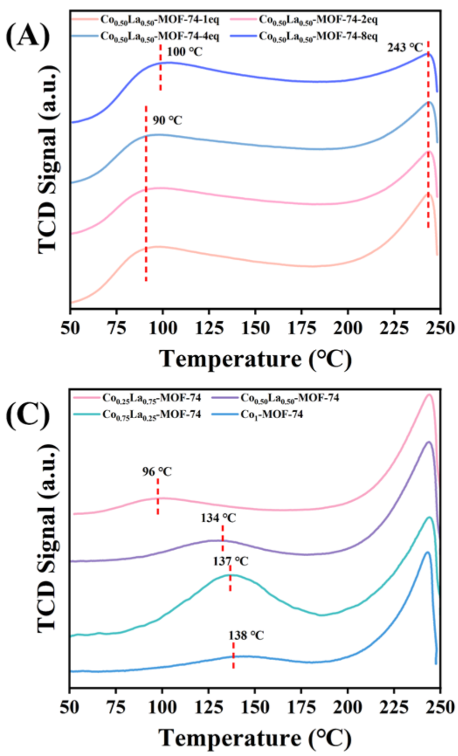

Figure S13. NH_3-TPD curves of (A) $Co_{0.50}La_{0.50}$-MOF-74-xeq, CO-TPD curves of (B) $Co_{0.50}La_{0.50}$-MOF-74-xeq, O_2-TPD profiles of (C) Co_xLa_{1-x}-MOF-74 and (D) $Co_{0.50}La_{0.50}$-MOF-74-xeq.

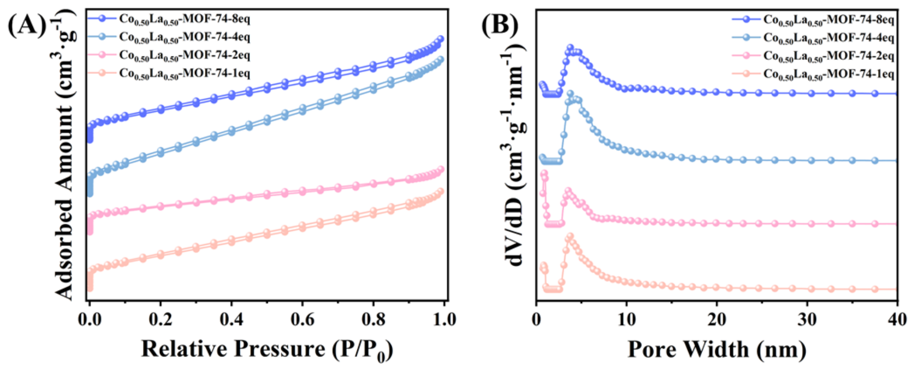

Figure S14. (A) 77 K N_2 adsorption-desorption isotherms, (B) pore size distribution curves of $Co_{0.50}La_{0.50}$-MOF-74-xeq.

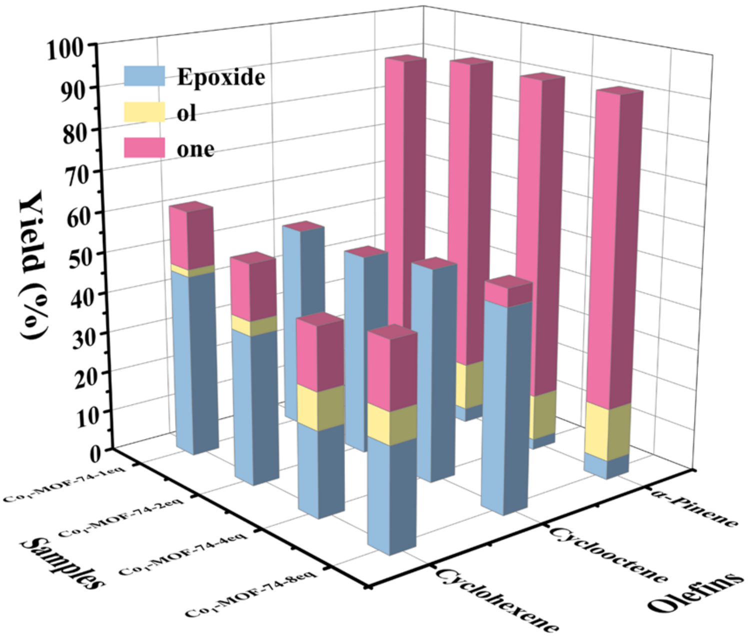

Figure S15. The catalytic performance catalyzed by Co$_1$-MOF-74-xeq for the epoxidation of cyclohexene, cyclooctene and α-pinene.

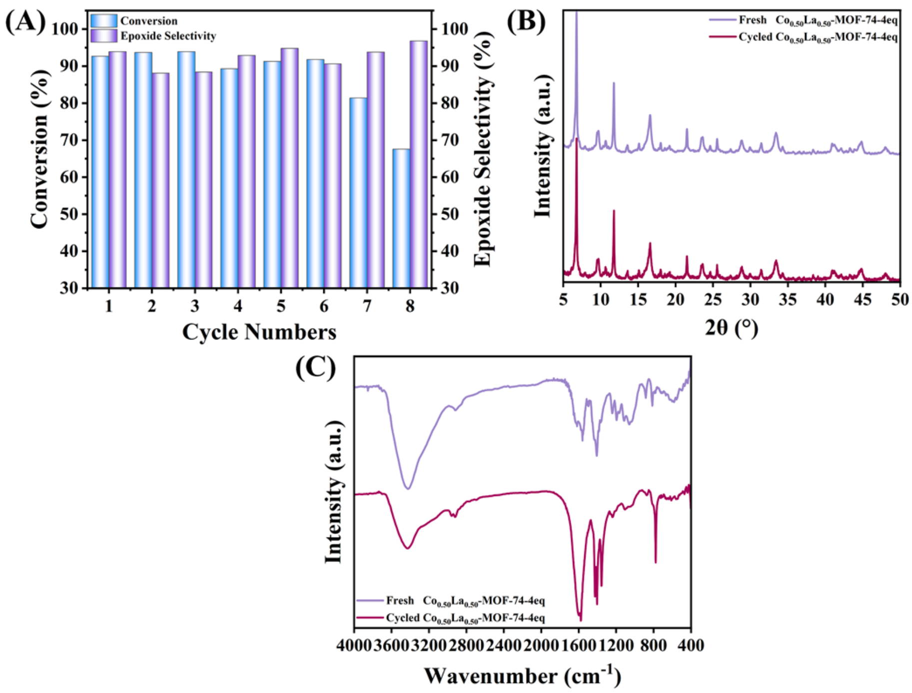

Figure S16. (A) The cycling stability experiments of $Co_{0.50}La_{0.50}$-MOF-74-4eq for cyclohexene epoxidation. (B) The XRD patterns and (C) The FT-IR spectra of fresh and cycled $Co_{0.50}La_{0.50}$-MOF-74-4eq.

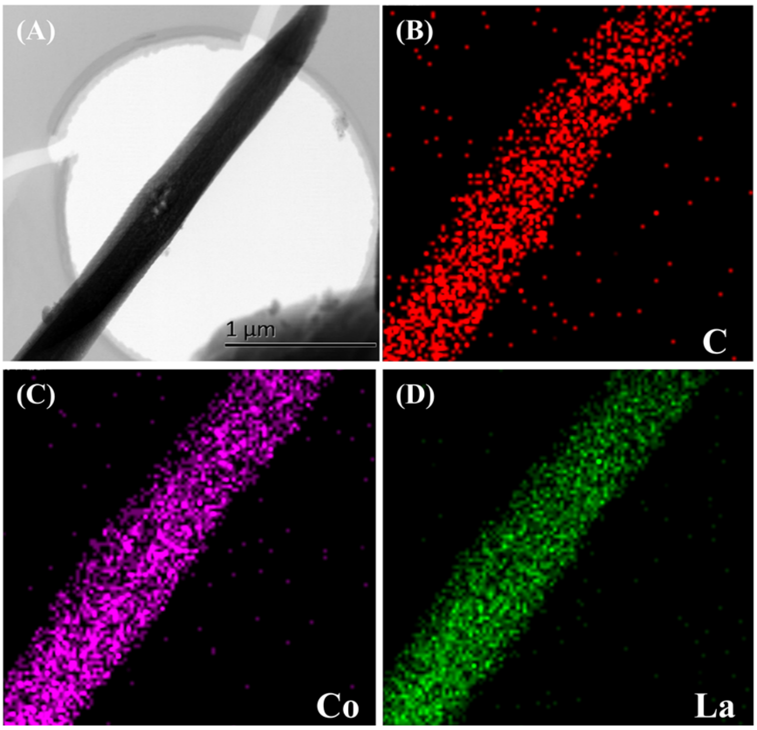

Figure S17. (A) TEM images of cycled $Co_{0.50}La_{0.50}$-MOF-74-4eq. Elemental mapping images of (C) C, (B) Co and (C) La elements.

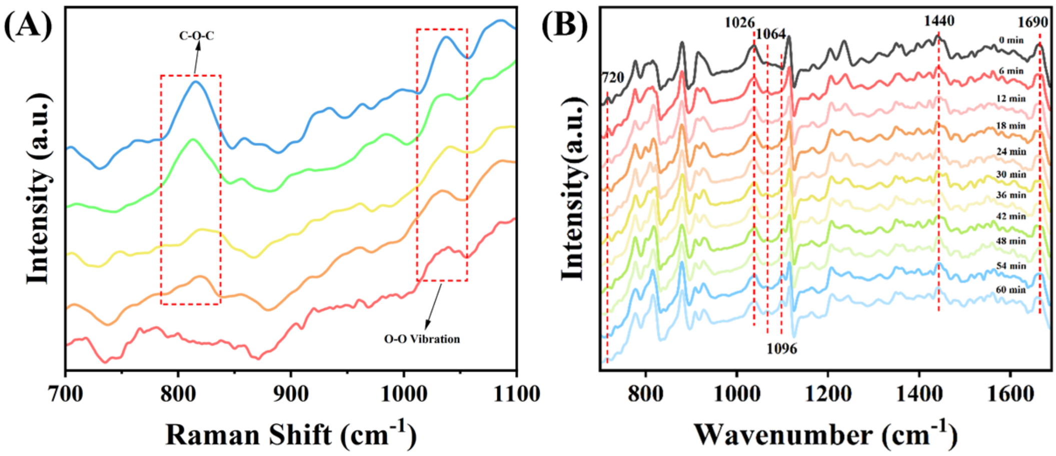

Figure S18. (A) In-situ Raman spectra in range of 700-1100 cm^{-1} and (B) In-situ FT-IR spectra in range of 700-1700 cm^{-1} over $Co_{0.50}La_{0.50}$-MOF-74-4eq.

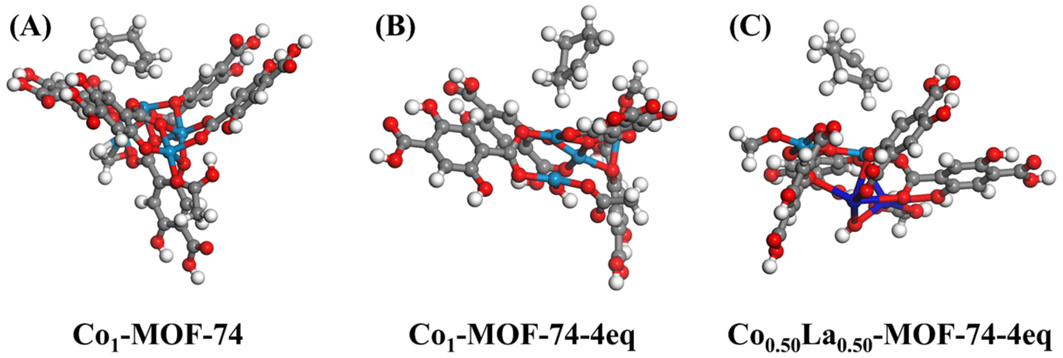

Figure S19. Adsorbed structural images of cyclohexene at metal sites of different catalysts.

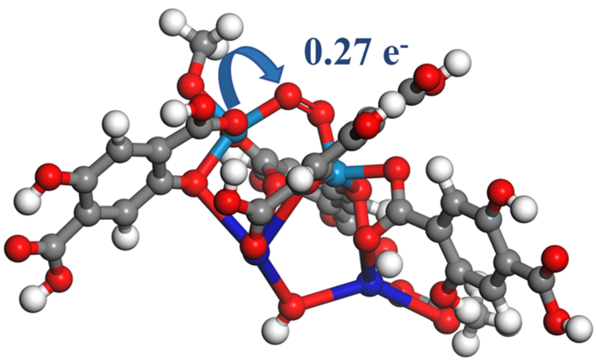

Mulliken Charge Transfer

Figure S20. The Mulliken charge transfer of $Co_{0.50}La_{0.50}$-MOF-74-4eq sample to O_2.

Table S1. Mass fraction and molar ratio of Co and La elements by ICP-OES in samples

Samples	Co (wt%)	La (wt%)	n_{Co} in 10 mg samples (mmol)	n_{La} in 10 mg samples (mmol)
Co_1-MOF-74	25.40	——	0.043	——
$Co_{0.25}La_{0.75}$-MOF-74	12.56	19.94	0.021	0.014
$Co_{0.50}La_{0.50}$-MOF-74	12.15	16.97	0.021	0.012
$Co_{0.75}La_{0.25}$-MOF-74	14.65	13.48	0.025	0.010
$Co_{0.50}La_{0.50}$-MOF-74-1eq	9.80	23.76	0.017	0.017
$Co_{0.50}La_{0.50}$-MOF-74-2eq	10.24	22.33	0.017	0.016
$Co_{0.50}La_{0.50}$-MOF-74-4eq	9.99	24.63	0.017	0.018
$Co_{0.50}La_{0.50}$-MOF-74-8eq	11.32	24.35	0.019	0.018

Table S2. Cellular parameters and Co^{2+}/Co^{3+} content of synthesized samples.

Samples	*a* ()	*b* ()	*c* ()	Volume (^{3})	Co^{2+}/Co^{3+} (%)
Co_1-MOF-74	26.13	26.13	6.72	3973.43	18.56
$Co_{0.75}La_{0.25}$-MOF-74	26.21	26.21	6.75	4015.65	15.90
$Co_{0.50}La_{0.50}$-MOF-74	26.24	26.24	6.79	4048.70	15.06
$Co_{0.25}La_{0.75}$-MOF-74	26.27	26.27	6.82	4075.89	20.80
$Co_{0.50}La_{0.50}$-MOF-74-1eq	26.28	26.25	6.78	4050.44	15.56
$Co_{0.50}La_{0.50}$-MOF-74-2eq	26.35	26.25	6.77	4055.24	25.33
$Co_{0.50}La_{0.50}$-MOF-74-4eq	26.26	26.28	6.80	4063.94	42.12
$Co_{0.50}La_{0.50}$-MOF-74-8eq	26.33	26.23	6.79	4061.04	17.03

Table S3. Mole percentage of DMF, DHBDC and HAc tested by [1]H NMR spectroscopy, and coordination number of $Co_{0.50}La_{0.50}$-MOF-74-xeq.

Samples	DHBDC (mol%)	DMF (mol%)	HAc (mol%)	coordination number (N)
$Co_{0.50}La_{0.50}$-MOF-74-1eq	83.3	15.0	1.7	5.49
$Co_{0.50}La_{0.50}$-MOF-74-2eq	76.5	19.9	3.6	5.47
$Co_{0.50}La_{0.50}$-MOF-74-4eq	76.1	17.5	6.3	5.20
$Co_{0.50}La_{0.50}$-MOF-74-8eq	52.2	41.7	6.1	4.13

Table S4. Microstructural properties of Co_xLa_{1-x}-MOF-74 and $Co_{0.50}La_{0.50}$-MOF-74-xeq.

Samples	S_{BET} [a] (m^2 g^{-1})	$S_{Micropore}$ [b] (m^2 g^{-1})	$S_{External}$ [b] (m^2 g^{-1})	Micropore Volume [b] (cm^3 g^{-1})	Mesopore Volume [c] (cm^3 g^{-1})
Co_1-MOF-74	409	0	409	0	0.566
$Co_{0.25}La_{0.75}$-MOF-74	601	250	351	0.125	0.304
$Co_{0.50}La_{0.50}$-MOF-74	257	23	234	0.006	0.307
$Co_{0.75}La_{0.25}$-MOF-74	488	185	303	0.099	0.360
$Co_{0.50}La_{0.50}$-MOF-74-1eq	218	32	186	0.018	0.167
$Co_{0.50}La_{0.50}$-MOF-74-2eq	159	40	119	0.021	0.134
$Co_{0.50}La_{0.50}$-MOF-74-4eq	299	13	286	0.007	0.330
$Co_{0.50}La_{0.50}$-MOF-74-8eq	202	26	176	0.010	0.238

[a] S_{BET} (total surface area) was calculated by BET method.

[b] $S_{Micropore}$, $S_{External}$ and Micropore Volume were calculated by t-plot method.

[c] Mesopore Volume was calculated by subtracting the micropore volume from the total pore volume.

Table S5. Detailed catalytic performance for cyclohexene epoxidation of synthesized samples.

Samples	Conv. (%)	Sel. (%)		
	cyclohexene	A	B	C
$Co_{0.25}La_{0.75}$-MOF-74	54.5	72.5	10.2	17.3
$Co_{0.50}La_{0.50}$-MOF-74	60.9	73.0	7.7	19.3
$Co_{0.75}La_{0.25}$-MOF-74	55.7	68.3	10.3	21.5
Co_1-MOF-74	50.8	62.0	12.3	25.7
$Co_{0.50}La_{0.50}$-MOF-74-1eq	74.9	81.1	0.0	18.9
$Co_{0.50}La_{0.50}$-MOF-74-2eq	76.4	83.9	0.0	16.1
$Co_{0.50}La_{0.50}$-MOF-74-4eq	92.2	93.9	0.0	6.1
$Co_{0.50}La_{0.50}$-MOF-74-8eq	70.1	82.2	0.0	17.8
Co_1-MOF-74-1eq	61.1	73.8	2.9	23.3
Co_1-MOF-74-2eq	53.9	68.0	6.6	25.4
Co_1-MOF-74-4eq	45.4	46.2	20.2	33.6
Co_1-MOF-74-8eq	48.7	51.6	15.6	32.8

A: 1,2-epoxycyclohexane, B: 2-cyclohexen-1-ol, C: 2-cyclohexen-1-one.

Reaction condition for olefin epoxidation: acetonitrile, 5 mL; cyclohexene, 1 mmol; trimethylacetaldehyde, 2mmol; O_2, 1 atm; catalyst, 10 mg; 40 ℃, 1 h.

Table S6. Detailed catalytic performance for cyclooctene epoxidation of synthesized samples.

Samples	Conv. (%)	Sel. (%)	
	cyclooctene	A	B
$Co_{0.25}La_{0.75}$-MOF-74	38.2	>99.9	——
$Co_{0.50}La_{0.50}$-MOF-74	70.2	>99.9	——
$Co_{0.75}La_{0.25}$-MOF-74	37.9	>99.9	——
Co_1-MOF-74	66.2	84.2	15.8
$Co_{0.50}La_{0.50}$-MOF-74-1eq	37.3	>99.9	——
$Co_{0.50}La_{0.50}$-MOF-74-2eq	75.8	>99.9	——
$Co_{0.50}La_{0.50}$-MOF-74-4eq	77.3	>99.9	——
$Co_{0.50}La_{0.50}$-MOF-74-8eq	67.9	>99.9	——
Co_1-MOF-74-1eq	50.7	>99.9	——
Co_1-MOF-74-2eq	49.5	>99.9	——
Co_1-MOF-74-4eq	52.1	>99.9	——
Co_1-MOF-74-8eq	53.4	91.8	8.2

A: 1,2-epoxycyclooctane, B: 2-cycloocten-1-one.

Reaction condition for olefin epoxidation: acetonitrile, 5 mL; cyclooctene, 1 mmol; trimethylacetaldehyde, 2mmol; O_2, 1 atm; catalyst, 10 mg; 40 ℃, 1 h.

Table S7. Detailed catalytic performance for α-pinene epoxidation of synthesized samples.

Samples	Conv. (%)	Sel. (%)		
	α-pinene	A	B	C
$Co_{0.25}La_{0.75}$-MOF-74	41.2	81.7	13.7	4.6
$Co_{0.50}La_{0.50}$-MOF-74	46.2	79.8	12.6	7.6
$Co_{0.75}La_{0.25}$-MOF-74	55.2	79.3	12.4	8.3
Co_1-MOF-74	70.5	2.4	9.8	87.8
$Co_{0.50}La_{0.50}$-MOF-74-1eq	27.7	81.8	11.7	6.5
$Co_{0.50}La_{0.50}$-MOF-74-2eq	67.0	81.9	11.9	6.2
$Co_{0.50}La_{0.50}$-MOF-74-4eq	95.7	91.0	4.4	4.6
$Co_{0.50}La_{0.50}$-MOF-74-8eq	95.3	85.8	8.6	5.6
Co_1-MOF-74-1eq	89.5	2.7	12.6	84.7
Co_1-MOF-74-2eq	92.1	3.7	12.7	83.6
Co_1-MOF-74-4eq	91.8	2.8	12.2	85.0
Co_1-MOF-74-8eq	92.1	5.0	14.0	81.0

A: 2,3-epoxypinane, B: verbenol, C: verbenone.

Reaction condition for olefin epoxidation: acetonitrile, 5 mL; α-pinene, 1 mmol; trimethylacetaldehyde, 2mmol; O_2, 1 atm; catalyst, 10 mg; 40 ℃, 1 h.

Table S8. Detailed catalytic data for cyclohexene epoxidation of cycling experiment using $Co_{0.50}La_{0.50}$-MOF-74-4eq as catalyst.

Cycle numbers	Conv. (%)	Sel. (%)
	cyclohexene	Epoxides
1	92.7	93.9
2	93.7	88.1
3	93.9	88.4
4	89.3	92.9
5	91.3	94.8
6	91.8	90.6
7	81.4	93.8
8	67.6	96.8

Reaction condition: acetonitrile, 5 mL; cyclohexene, 1 mmol; trimethylacetaldehyde, 2mmol; O_2, 1 atm; $Co_{0.50}La_{0.50}$-MOF-74-4eq, 10 mg; 40 °C, 1 h. Catalyst mass loss was neglected during the reaction.

Table S9. Comparison of cyclohexene epoxidation catalyzed by $Co_{0.50}La_{0.50}$-MOF-74-4eq in this work with the reported catalytic performance.

Entry	Samples	Oxidant	Solvent	T (°C)	Time (h)	Yield (%)	Reference
1	$Co_{0.50}La_{0.50}$-MOF-74-4eq	O_2	CH_3CN	40	1	86.6	This work
2	NENU-MV-1a	Air	CH_3CN	35	2	81.7	[1]
3	Co-PTC	O_2	dichloromethane	35	10	58.1	[2]
4	Cu^{2+}@COMOC-4	O_2	chloroform	40	7	43.6	[3]
5	Mo@UiO-66-100for	H_2O_2	CH_3CN	60	2	~60	[4]
6	Co-NNO-MOF(48)	Air	CH_3CN	25	8	84.7	[5]
7	Co(II)@Cr-MIL-101-P2I	Air	CH_3CN	35	5	73.3	[6]
8	$Co_{51.8}Mo_{48.2}$-ZIF	TBHP	dichloroethane	80	20	83.8	[7]

Table S10. Detailed ALIE value of synthesized samples.

Samples	ALIE value	
	Min(eV)	Max(eV)
Co_1-MOF-74	6.40	16.43
Co_1-MOF-74-4eq	6.49	17.38
$Co_{0.50}La_{0.50}$-MOF-74-4eq	5.15	26.53

Table S11. Bond length of adsorbed oxygen of different samples.

Bond length ()	Original	Co_1-MOF-74	Co_1-MOF-74-4eq	$Co_{0.50}La_{0.50}$-MOF-74-4eq
O-O	1.22	1.27	1.25	1.38

Table S12. Adsorption energy of oxygen and cyclohexene at Co sites of different samples.

Absorb energy(eV)	Co_1-MOF-74	Co_1-MOF-74-4eq	$Co_{0.50}La_{0.50}$-MOF-74-4eq
O_2-Co	-1.98	-0.34	-3.02
Cyclohexene-Co	-0.99	-0.55	-0.98

Table S13. ΔG in the epoxidation pathway and the allylic oxidation pathway at 313.15 K.

ΔG of epoxidation pathway			ΔG of allylic oxidation pathway		
Products	HF (a.u.)	eV	Products	HF (a.u.)	eV
R($2C_6H_{10}+O_2$)	0	0	R($2C_6H_{10}+O_2$)	0	0
TS1	0.01	0.29	TS2	0.01	0.32
M1($2C_6H_{10}O$)	-0.05	-1.49	M2(C_6H_9-OOH+C_6H_{10})	0.003	0.08
			TS3	-0.08	-2.04
			M3($C_6H_{10}O+C_6H_9$-OH)	-0.09	-2.53

References

1 S. Wang, Y. Liu, Z. Zhang, X. Li, H. Tian, T. Yan, X. Zhang, S. Liu, X. Sun, L. Xu, F. Luo and S. Liu, *ACS Appl. Mater. Interfaces*, 2019, **11**, 12786-12796.

2 X. Sun, L. Wang and Z. Tan, *Catal. Lett.*, 2015, **145**, 1094-1102.

3 Y. Y. Liu, K. Leus, T. Bogaerts, K. Hemelsoet, E. Bruneel, V. Van Speybroeck and P. Van Der Voort, *ChemCatChem*, 2013, **5**, 3657-3664.

4 M. Jin, G. Liu, C. Si, Z. Lv, X. Cheng, H. Han and Q. Niu, *Mol. Catal.*, 2022, **524**, 112312.

5 Y. Qin, B. Wang, J. Li, X. Wu and L. Chen, *Transition Met. Chem.*, 2019, **44**, 595-602.

6 J. Wang, M. Yang, W. Dong, Z. Jin, J. Tang, S. Fan, Y. Lu and G. Wang, *Catal. Sci. Technol.*, 2016, **6**, 161-168.

7 W. Zou, Y. Guo, P. Li, M. Liu and L. Hou, *ChemCatChem*, 2020, **13**, 416-424.